IADC-08-03
Version 2.1
April 2013

Inter-Agency Space Debris Coordination Committee

SENSOR SYSTEMS TO DETECT IMPACTS ON SPACECRAFT

Action Item 22.3

Prepared by the IADC WG3 members

Change Record

Issue / Revision	Date	Chapter	Change(s)	Contributor
0.1	13.04.06	All	Issue of doc. v0.1 during WG Session 3.3 of IADC 24	F. Schaefer / WG3
0.2	27.06.07	All	Issue of doc. v0.2 prior to start of IADC25 meeting in Toulouse	H. Stokes / WG3
0.3	22.08.07	All	Issue of doc. v0.3 after discussions at IADC25 meeting in Toulouse	H. Stokes / WG3
0.4	31.01.08	All	Issue of doc. v0.4 after receipt of the following inputs from WG3 authors and reviewers: – Revised text in 2.2, 3.2, 3.3, 3.5, 3.8, 3.9, 3.10, 4, Appendices – New text in 3.4, 3.11, 3.12, 3.13	H. Stokes / WG3
0.5	07.04.08	All	Issue of doc. v0.5 after receipt of the following inputs from WG3 authors and reviewers: – Revised text in 2, 3, 6, Appendices – New text in 4, 5, 7	H. Stokes / WG3
1.0	16.04.08	All	Issue of doc. v1.0 to Steering Group after receipt of final inputs and review at IADC26	WG3
1.0	26.08.09	3	Deleted 3.8 thru 3.11 (approved by SG)	WG3
1.1	30.11.10	2	Updated per IT28-2-2, Removed impacting particle type, size or mass, speed and direction in Table 2.3-1. Completely revised section 2.5	K. Nagy H. Stokes
2.0	08.09.11 09.06.12	All	Formatting edits Submitted to SG	D. Nikanpour
2.1	18.04.13	Scope	Inserted “health monitoring”	M. Higashide

Table of Contents

List of Figures

List of Tables

Scope

The scope of this document is to assess the possibilities for developing and implementing impact sensor systems on spacecraft. The purpose of these systems is spacecraft health monitoring. As a health monitoring system, the sensors provide data to determine if micro-meteoroid and orbital debris impact is the cause of a spacecraft anomaly.

Summary

This document lists the different techniques for impact damage detection on spacecraft. It addresses the technical feasibility of different options for detecting and characterizing impacts (e.g. those exceeding a certain energy and/or momentum threshold) and those suitable for determining if meteoroid/debris impacts are affecting the health and status of spacecraft (e.g. by detecting the number, location and severity of meteoroid/debris impacts)

In this report, the different sensor system options are described, including:

- general schematic of sensor system
- pros and cons of each option
- mass/volume/power anticipated for deployment on spacecraft
- description of the efforts for integration of the sensor option into a spacecraft
- description of the development status and technology readiness level
- information whether smaller/similar systems have been used as science payloads on spacecraft, or on non-space vehicles
- description of what work is going on and where

1 Introduction

1.1 Background and Motivation

Inspection of retrieved spacecraft has illustrated the presence and to some extent the effects of meteoroids and space debris on space vehicles [Mullen, 1993]. There is a growing need for a better understanding of the interaction of space debris with space systems. This is crucial for the design and the survival of space missions especially where human safety is concerned. Indeed, surface damage resulting from the impact of several small particles (less than 1 mm), which individually are not lethal for a spacecraft, may become one of the major concerns for sensitive devices used in space (optics, thermal control coatings, solar cells) especially for long term missions. Moreover, meteoroid streams can produce poorly known damage. In the case of brittle materials, impact ejecta from both sides of a surface could a) lead to internal damage, b) interact with other areas of the structure, and c) increase the total debris population. Over the past few years, several spacecraft missions have flown sensors devoted to the monitoring of this particular environment [Berthoud, 1993; Simon *et al*, 1993]. However most of the detectors consist of passive surfaces, retrieved after their exposure to space. In these conditions, most of the data obtained were limited to low earth orbits. Moreover, a few active experiments did indicate a non-random distribution of particles, in space and in time [Maag, 1996; Simon *et al*, 1993]. In recent years, several organisations have been involved in the development of active detectors, which could be used for real-time monitoring of small orbital debris.

This report discusses the possibilities for developing and implementing sensor systems to detect critical and non-critical impacts on spacecraft (i.e. instrumenting the entire spacecraft) and large-scale structures. Included are the different techniques for impact damage detection on spacecraft. The technical feasibility of different options for detecting and characterizing impacts (e.g. by detecting the number, location and severity of meteoroid/debris impacts) is also addressed.

1.2 Problems of Impacting Particles

Spacecraft operate in a meteoroid environment and, for the ones in earth orbits, a space debris environment. This includes crewed spacecraft and satellites. There are significant probabilities of impact on the spacecraft. High energy impacts may cause very extensive damage to spacecraft systems. The damage could pose risks to crew, resulting in loss of life. The damage could result in loss of spacecraft subsystems. This would result in reduced capability such as less available power or thermal conditioning capacity, etc. In order to monitor the effects from impact of MMOD particles on the spacecraft, it is highly desired to include a sensor system in the design of the spacecraft, especially for crewed spacecraft.

- Risk of penetration cannot be completely eliminated by current technology, especially considering long duration missions.
- Considering crew evacuation and the possibility of a repair operation by the crew, identifying the location and severity of the debris impact is an indispensable requirement especially for manned systems, such as the International Space Station.

- Although, so far, many kinds of impact detectors or impact sensors using different principles have been proposed and developed for various missions (especially scientific missions), an Impact Monitoring System for spacecraft health monitoring has quite different system requirements from impact detectors, which typically are science payloads with limited active area.
- The system must cover a very wide area on the surface of the space system and is required to provide a quick alert if major damage is detected.
- Sensors integrated on board spacecraft for general health monitoring can also be used for impact damage assessment.
- In addition, implementation in the actual system requires a lot of consideration from a viewpoint of actual structural configuration, signal transfer and etc.

1.3 References

Berthoud, L., *Micrometeoroids and orbital debris observed in low earth orbits*, PhD Thesis ENSAE, Toulouse, 1993. (NB. This is not an easily accessible reference)

Maag, C., *Debris clouds indicated by ESEF data from MIR*, SFE Newsletter, 7,1, 1996.

Mullen, S., et al., *A study of meteoroids and debris impacts on the LDEF UHCRE thermal blankets*, First European Conference on Space Debris, Darmstadt, Germany, ESA SD-01, 5-7 April 1993.

Simon, G., et al., *Long term microparticle flux variability*, NASA CP 3194, 1993.

2 Characterization of Impacts on Spacecraft

2.1 Description of Physical Effects of Impacts

A hypervelocity impact is characterised by the following measurable effects:

- electromagnetic emissions (e.g. visible light flash, infra-red radiation, and microwave radiation)
- acoustic emissions (within the impacted structure)
- secondary debris clouds and ejecta
- plasma clouds
- shock-induced accelerations
- size and shape of crater or hole
- chemical properties of crater material residue

2.2 Consequences of Impacts

The consequences of a hypervelocity impact on a spacecraft are dependent on the characteristics of the impactor (such as mass and velocity), the location of the impact, and the design of the spacecraft. Therefore, a wide range of effects is possible, and the consequences can range from negligible to mission-terminating. The dependence of damage effects on impactor size is summarised in Table 2.2-1 [Drolshagen, 2005].

Minimum particle size for which effect is noticeable	Effect
< 1 µm	No or little individual effect. Some surface degradation (sandblasting effect) leading to a change of thermal, optical or electrical properties.
1 µm	Temporary saturation and permanent damage of exposed CCD pixels (e.g. for x-ray telescopes). Degradation of mirrors and sensors by direct impacts and by secondary ejecta. Penetration of outer coatings and surface layers allowing subsequent attack of other environment components (plasma, Atomic Oxygen). Triggering of electrostatic discharges of pre-charged surfaces (effect demonstrated but minimum particle size still uncertain). Creation of new small debris by ejecta.
10 µm	Noticeable individual craters, e.g.: • craters visible to naked eye (> 200 µm) on brittle surfaces (glass) • potential sealing problem of exposed hatches Effects of momentum transfer (which can be 5-20 times larger than the incoming momentum because of secondary ejecta) leading to: • disruption of stable attitude • disturbance of formation flying Electromagnetic interference from impact plasma. Optical light flash. Impact generated radio waves.

Minimum particle size for which effect is noticeable	Effect
100 µm	Noticeable damage on sensitive sensors and surfaces (Shuttle windows require replacement). Cutting of thin tethers, springs, wires. Penetration of MLI. Penetration of 300-500 µm wall thickness. Penetration of heat pipes, coolant loops, radiators. Penetration of solar cells (short circuits, arc burning).
1 mm	Craters/holes from 2mm to 1 cm in diameter or larger depending on type and thickness of material impacted. Penetration of 3-5 mm wall thickness with damage on equipment behind wall. Structural damage of exposed equipment. Penetration of tanks, baffles, sun-shields, external cables, etc.
1 cm	Structural damage/ destruction on any spacecraft part hit. Penetration of all shields, including special protection of manned modules. Creation of many new large debris pieces.
10 cm	Complete destruction of satellite or subsystem hit. Interference with astronomical observations.
1 m	Solid spacecraft parts can survive re-entry and hit ground.

Table 2.2-1 Dependence of hypervelocity impact damage effects on particle size (Note: larger particles usually have all the effects listed under the smaller sizes as well)

Debris objects smaller than ~0.1 mm in size represents a very low penetration hazard to a spacecraft, but because the population of such objects is so large in LEO (several orders of magnitude greater than the trackable population), multiple impacts can occur. Over the mission life these impacts can cause an accumulation of minor damage to spacecraft surfaces, such as surface pitting and erosion. Evidence for this has been gathered from several missions for which exposed surfaces on spacecraft such as LDEF, EURECA, and HST have been retrieved from space and examined. These showed significant numbers of small impact craters; in the case of LDEF more than 30,000 were observed. However, there was no discernible effect on the missions.

Synergistic environmental effects are another potential cause of damage to a spacecraft [Lu & Nahra, 1991]. For example, multiple small debris impacts can erode atomic oxygen (AO) protective coatings thereby allowing AO impingement. The material released from the resulting oxygen ion sputtering could then be a source of contamination.

For debris in the 0.1 mm to 10 mm size range, significant structural damage can occur. This might include penetration of exposed instruments located on the outside of a spacecraft. Penetration of the structure and damage to internal equipment is another distinct possibility. Both effects could lead to partial or complete loss of a mission. Christiansen *et al* (1993) have also shown that a homogeneous particle impacting a spacecraft surface at a highly oblique angle (> 65° with respect to the surface normal) can cause the particle to break-up and release fragments that are projected onto other surfaces, or back into space. A mathematical model of this ejecta phenomenon has been derived by Rival & Mandeville (1999).

It is generally considered unlikely that a spacecraft will survive an impact with a particle larger than ~10 mm, if the impact occurs on or near a critical system, mainly because of the penetrative damage caused. At the very least, the transfer of momentum may cause the spacecraft to lose attitude control. If the debris object is large enough, the post-impact stress waves could carry sufficient energy through the structure to cause a catastrophic break-up of a spacecraft. For this to occur, the ratio of impact energy to spacecraft mass has to exceed a certain value. As a 'rule-of-thumb' a figure of 40 J / gram has been suggested [US National Research Council, 1995].

To understand further the consequences of an impact on a spacecraft, Table 2.2-2 lists some of the damage effects that typical subsystems might experience.

Subsystem	Possible impact effects	References
Honeycomb panels (Carbon Fibre Reinforced Plastic (CFRP) facesheets, Aluminium honeycomb)	Hole through facesheet: • Delamination around hole • Reduced electromagnetic compatibility Honeycomb blast damage: • Thermal distortion stresses • Thermal conductive paths disrupted Release of ejecta and cloud: • Damage to equipment both inside and outside the spacecraft	Taylor *et al* (1997) Turner *et al* (1999)
Solar panels	Sub-millimetre impactors can cause: • Erosion of surface coating • Cracking of cover glass • Penetration of cell • Reduction of light energy transmission • Severed wire leading to loss of cell string or circuit • Production of plasma cloud, possibly leading to electro-static discharge and circuit burn-out	Gurule *et al* (1992) McDonnell *et al* (1997) Caswell (1998)
Pressure vessels / tanks (For storing propellant at low pressure, or storing inert gas at high pressure)	• Stress concentration around entry hole can cause front side failure • Spall fragments in liquid / gas contaminate tank, pipes, pumps • Fragments can crater and perforate rear wall, and lead to crack growth and wall failure • Transmission of shock wave through liquid / gas can impact rear wall causing bulge or failure • Catastrophic rupture occurs when vessel is above a critical pressure • A very reactive liquid may ignite, decompose or detonate	Schäfer *et al* (1997) Lambert (1990) Poe & Rucker (1993)
Steering/pointing mechanisms	Spall fragments released into motor casing may cause motor to jam	
Electrical harness	Severed wires causing open-circuit, or grounded shields can come in contact with conductor causing short-circuit (or current isolation)	

Subsystem	Possible impact effects	References
Manned pressurised modules	Failure modes caused by penetration: • Crack growth in module wall, leading to module rupture and decompression • Uncontrolled thrust from air leak, leading to loss of attitude control and structural failure • Damage to critical internal equipment • Injury to crew from fragments, heat, light-flash, and over-pressure • Hypoxia-induced crew unconsciousness and eventual loss (especially if hole is large, i.e. depressurisation is rapid) • Fire	Williamsen & Schonberg (1997) Destefanis & Callea (1993)
Windows / viewports	Impact on brittle glass produces a large area of radial and concentric cracking, thus reducing visibility. Visibility improved if glass is strengthened with acrylic or polycarbonate in a sandwich configuration	Lambert (1990)

Table 2.2-2 Possible hypervelocity impact damage effects on spacecraft subsystems

The extent to which a spacecraft is disrupted by an impact is driven by a number of design factors, for example:

- The function and criticality of the spacecraft subsystems
- The level and distribution of any redundancy
- The robustness of structures and equipment to withstand impacts
- The location and alignment of equipment and instruments relative to the debris flux direction

Any decision to incorporate an impact sensor system into a spacecraft must therefore take account of these factors.

2.3 Requirements on Sensor System

The requirements listed below are examples of typical requirements on sensor systems:

1. The sensor systems have to be able to function under all of the imposed environmental conditions that it is exposed to on the spacecraft. This includes thermal, vibration, shock, structural loading, radiation, etc.
2. The sensor systems have to be integrated with the spacecraft subsystems. This includes power system, software system, thermal conditioning, etc. The sensor system integration may be performed as part of the original design and build of the spacecraft. However for existing spacecraft such as International Space Station the sensor systems may be retrofitted into existing spacecraft elements.
3. The sensor systems have to be calibrated. This includes initial calibration as well as periodic recalibration.
4. The sensor systems have to meet applicable crew systems requirements for crewed spacecraft. This includes requirements for system operation as well as system maintenance.

5. The sensor systems have to be designed to minimize the use of spacecraft resources, such as allocation for surface area, volume, mass, power, thermal, data bandwidth, etc.
6. The sensor systems have to be designed to detect well defined failure criteria for spacecraft systems, and only report impacts that result in damage exceeding those failure criteria (to minimize false alarms).
7. The sensor systems have to be designed to well-defined criteria for accuracy on the location of the impact damage that is detected by the sensors.
8. The sensor systems have to be designed to provide impact data for all of the critical surfaces of the spacecraft.

Table 2.3-1 provides a list of requirements that a sensor system might satisfy if it is to be considered for implementation on typical spacecraft.

Broad requirements	Detailed requirements	Crewed Space Vehicles	Crewed Re-entry Vehicles	Unmanned LEO Satellites	Unmanned GEO Satellites
What to measure/sense	Impact energy	Yes	Yes	Yes	Yes
	Impact time	Yes	Yes	Yes	Yes
	Impact location	Yes	Yes	Yes	Yes
	Impact crater/hole size	Critical damage to pressure shell (for example: any size through hole)	Critical damage to thermal protection system	??	??
Accuracy of measurements	Impact energy	TBD	TBD	TBD	TBD
	Impact time	+/- 1 minute	+/- 1 minute	+/- 1 minute	+/- 1 minute
	Impact location	+/- 10 cm	+/- 10 cm	+/- 10 cm	+/- 10 cm
	Impact crater/hole size	+/- 0.5 mm	+/- 1 mm	??	??
Average demand on spacecraft	Comprises factors such as sensor system mass, volume, power, data (size, rate), reliability, software	< 1% S/C total	< 1% S/C total	< 1% S/C total	< 1% S/C total
Environmental constraints	Temperature range	-70° to +50°C	-150° to +70°C	-70° to +50°C	-150° to +70°C
	Degradation over life	< 10%	< 10%	< 20%	< 20%
	Vibration tolerance	? (launcher)	? (launcher)	? (launcher)	? (launcher)
	EMC	No interference	No interference	No interference	No interference
	Radiation tolerance	?	?	?	?
	Charging	?	?	?	?
	Contamination	None	None	None	None
	Emissions	None	None	None	None
Ease of integration and use	Comprises factors such as assembly, integration, calibration, testing, operations, maintenance	< 1% S/C total	< 1% S/C total	< 1% S/C total	< 1% S/C total
Recurring cost		< 1% S/C total	< 1% S/C total	< 1% S/C total	< 1% S/C total
Coverage on spacecraft	Whole spacecraft or specific elements / modules	Crew modules	Thermal protection system on descent module	Service & P/L modules (mainly high risk surfaces)	Service & P/L modules (all surfaces)

Table 2.3-1 Sensor system requirements

2.4 Other Vehicle Requirements/Constraints that Support Use of Sensors

Sensors are useful for detecting and locating critical damage, but MMOD risk reduction depends on the presence of other systems or operational procedures to mitigate the risk after damage is detected/located. This section describes requirements for other vehicle systems and operations that support MMOD risk reduction using sensors.

2.4.1 Procedures and design requirements to mitigate risk if MMOD damage detected

2.4.1.1 Crewed vehicles

- Provide for inspection of damaged area via optical scanners, cameras or crew
- Define procedures for isolating leaks
- Develop and carry patch kits for temporary repair and permanent repair of leaks in pressure shell
- Develop and carry repair kits for thermal protection system (TPS) of re-entry vehicles
- Provide for EVA and IVA access to the pressure shell
- Provide means for conducting non-destructive evaluation of damage in the pressure shell
- Provide replacements (spares) for damaged items

2.4.1.2 Unmanned vehicles

- Include means and define procedures for isolating leaks in propellant tanks and gas/liquid systems
- Provide redundancy
- Provide fail-safe systems

2.5 Post-Impact Assessment Issues

The basic requirement for a sensor system requires that it is designed to locate the point of impact on the spacecraft. It is expected that over the lifetime of the spacecraft many impacts are detected. However only a small portion of those impacts are going to cause critical damage to spacecraft systems. This implies the need for the development of threshold damage requirements for the spacecraft components, such that the sensor system only records those impacts that result in unacceptable damage. The development of spacecraft component failure criteria due to MMOD impact requires extensive testing and analysis of the component hardware. For example for ISS MMOD shots were performed for electrical and data cables, fluid lines, electronic hardware, etc. to aid in the development of failure criteria.
The failure criteria for spacecraft components are very much a function of the particular spacecraft configuration, the MMOD protection and the design of the components.
Analysis has to be performed for the hardware mounted on the spacecraft to determine the probabilities of damage using the failure criteria that was obtained from testing.

An impact on a spacecraft may cause damage to multiple components. Each of those components would have different failure criteria, with different threshold values. An impact of a particular severity could result in multiple spacecraft component failures.

Impact sensor systems have a basic inherent limitation. The location and time of the impact can be detected. The magnitude of the impact energy may be inferred from the detected signal amplitudes. However the path of the impacting particle within the spacecraft structure and the depth of penetration of the particle into the spacecraft can only be determined by disassembly and detailed inspection of the damaged area. This may be feasible for portions of a crewed spacecraft on orbit, but it cannot be performed for an unmanned spacecraft without the return of that spacecraft from orbit.

The limitations of impact sensor systems can be mitigated by monitoring the functionality of the various components in the spacecraft. The basic design of each system includes some means of monitoring system parameters, such as current, temperature, data flow, etc. In the event of damage to a system those parameters will change. Some of the systems also may include in situ diagnostic capability to indicate what failures occurred within the system.
In the event of an indicated MMOD strike, all of the system data for the systems on that spacecraft would have to be assessed if any failures are indicated.

An option for impact sensor system design is that the threshold value for the sensor system can be set at a minimum value that would result in the penetration of the spacecraft shielding. When an impact is detected and located that occurred above this threshold value, then the specialists for each spacecraft system are required to assess the functionality of the individual system using the measured system parameters. This would result in a simpler sensor system development, without the need for development of detailed failure criteria due to MMOD impact for each component.

2.6 References

Caswell, D., *Olympus and the 1993 Perseids: Lessons for the Leonids*, Leonids Threat Conference, Manhattan Beach, April 26/271998.

Christiansen, E.L., Cykowski, E., and Ortega, J., *Highly Oblique Impacts into Thick and Thin Targets*, International Journal of Impact Engineering, Vol. 14, pp. 157-168, 1993.

Destefanis, R., and Callea, M., *Meteoroid and Debris Impacts on Orbiting Structures: A Methodology*, Proceedings of the First European Conference on Space Debris, Darmstadt, ESA SD-01, pp. 523-533, 1993.

Drolshagen, G., *Effects of hypervelocity impacts from meteoroids and space debris*, ESA TEC-EES/2005.302/GD, 28 June 2005.

Gurule, A.P., Yates, K.W., and Evans, R.M., *Impact of Space Debris on Solar Photovoltaic Array Performance*, IAF paper 92-0335, presented at the 43rd International Astronautical Congress, Washington, USA, September 1992.

Lambert, M., *Shielding against Orbital Debris – A Challenging Problem*, In: Proc. ESA Symp.: 'Space Applications of Advanced Structural Materials', ESTEC, Noordwijk, ESA SP-303, June 1990.

Lu, C-Y., and Nahra, H.K., *Assessment of environmental effects on Space Station Freedom Electrical Power System*, In: Proceedings of the 26th Intersociety Energy Conversion Engineering Conference, Boston, MA, Vol. 1, pp. 374-379, August 1991.

McDonnell, J.A.M., McBride, N., and Gardner, D.J., *The Leonid Meteoroid Stream: Spacecraft Interactions and Effects*, Proceedings of the Second European Conference on Space Debris, Darmstadt, ESA SP-393, pp. 391-396, May 1997.

Poe, R.F., and Rucker, M.A., *Evaluation of Pressurized Vessels following Hypervelocity Particle Impact*, Proceedings of the First European Conference on Space Debris, Darmstadt, ESA SD-01, pp. 441-446, 1993.

Rival, M., and Mandeville, J.C., *Modeling of Ejecta Produced upon Hypervelocity Impacts*, *Space Debris*, Vol. 1, No. 1, pp. 45-57, 1999.

Schäfer, F., Schneider, E., and Lambert, M., *An Experimental Study to Investigate Hypervelocity impacts on Pressure Vessels*, Proceedings of the Second European Conference on Space Debris, Darmstadt, ESA SP-393, pp. 435-443, May 1997.

Taylor, E.A., Herbert, M.K., and Kay, L., *Hypervelocity Impact on Carbon Fibre Reinforced Plastic (CFRP)/Aluminium Honeycomb at Normal and Oblique Angles*, Proceedings of the Second European Conference on Space Debris, Darmstadt, ESA SP-393, pp. 429-434, May 1997.

Turner, R., Berthoud, L., Griffiths, A.D., McDonnell, J.A.M., Marriott, P., Stokes, P.H., Taylor, E.A., and Wilkinson, J.E., *Cost-Effective Debris Shields for Unmanned Spacecraft: Final Report*, Issue 1, Submitted to ESA under Contract No. 12378/97/NL, December 1999.

US National Research Council (Committee on Space Debris), *Orbital Debris – A Technical Assessment*, ISBN 0-309-05125-8, National Academy Press, 1995.

Williamsen, J., and Schonberg, W., *Empirical Models for Spacecraft Damage from Orbital Debris Penetration and Effects on Spacecraft Survivability*, Proceedings of the Second European Conference on Space Debris, Darmstadt, ESA SP-393, pp. 519-525, May 1997.

3 Detection of Impacts on Spacecraft

The following impact sensor / monitoring techniques are documented in this chapter:

- Acoustic emission
- Acceleration for impact shock detection
- Impact detection using thermography
- Calorimetry
- Fibre optic impact sensors
- Resistor-based detection
- Microwave emission
- Surface inspection cameras

Each of these techniques is described according to the following sub-chapter structure:

1. Sensor description
2. Sensor development status
3. Sensor measurement capability
4. Demands on the spacecraft
5. Environmental robustness
6. References

Technical data on the different techniques are also provided in Appendices A to G.

3.1 Acoustic Emission

3.1.1 Sensor description

Acoustic Emission (AE) is the class of phenomena whereby an elastic wave, in the range of ultrasound usually between 20 KHz and 1 MHz, is generated by the rapid release of energy from the source within a material. The elastic wave propagates through the solid to the surface, where it can be recorded by one or more sensors. The sensor is a transducer that converts the mechanical wave into an electrical signal. In this way information about the existence and location of possible sources is obtained. The basis for quantitative methods is a localization technique to extract the source coordinates of the AE events as accurately as possible.

AE differs from ultrasonic testing, which actively probes the structure; acoustic emission listens for emissions from active defects and is very sensitive to detect activity when a structure is loaded beyond its service load in a proof test.

AE analysis is a useful method for the investigation of local damage in materials. One of the advantages compared to other NDE techniques is the possibility to observe damage processes during the entire load history without any disturbance to the specimen. [Dae-Un Sung *et al*, 2002].

AE analysis is used successfully in a wide range of applications including: detecting and locating faults in pressure vessels or leakage in storage tanks or pipe systems, monitoring welding applications, corrosion processes, partial discharges from components subjected to high voltage and the removal of protective coatings. Areas where research and development of AE applications is currently being pursued, among others, are process monitoring and global or local long-term monitoring of civil-engineering structures (e.g., bridges, pipelines, off-shore platforms, etc.). Another area where numerous AE applications have been published is fibre-reinforced polymer-matrix composites, in particular glass-fibre reinforced parts or structures. (e.g. fan blades). AE systems also have the capability of detecting acoustic signals created by leaks.

The disadvantage of AE is that commercial AE systems can only estimate qualitatively how much damage is in the structure and approximately how long the components will last. So, other NDE methods are still needed to do more thorough examinations and provide quantitative results. Moreover, service environments are generally very noisy, and the AE signals are usually very weak. Thus, signal discrimination and noise reduction are important points to be assessed in any new application, and extremely important for successful AE applications in the health monitoring of spacecraft.

3.1.2 Sensor development status

For researchers in the area of nondestructive detecting, localization with acoustic emission has become a point of interest. Various methods have been studied and used to locate the active faults in many different fields. [Promboo, 2000; Chen, 2002].

AE techniques performances have been assessed by various institutions. The application of the AE in the ESA Columbus Module were carried out in the early 1990's by Det Norske Veritas in two ESA contracts [Norske Veritas, 1992]. The feasibility of the technique was demonstrated by tests on a full scale structure.

In Australia, CSIRO has been developing an AE-based Aerospace Structural Health Management sensor system for the AAV Concept Demonstrator satellite [Price, 2005].

Schafer & Janovsky (2002) investigated the source location and impact signals of a 2 mm thick Al-alloy panel and a 49 mm thick Al-honeycomb sandwich panel. They gave the impacting location comparison results between the prediction and the test for the impact, the location accuracy of the Al-alloy panel is better than that of Al-honeycomb due to the different material property. Recently, new types of acoustic emission based sensor, which have improved performance compared to conventional AE sensors, have been studied. [Finkel *et al*, 2001].

Madaras *et al* (2005) describe application of AE techniques to detect impact damage to the NASA Space Shuttle orbiter vehicle.

3.1.3 Sensor measurement capability

High sensitivity of AE techniques make it is easy to detect sub-millimetre size particle impact, and many kinds of damage modes such as defects, flaws, cracks etc. can be

distinguished early and rapidly. Another advantage of AE techniques are the real time monitoring, global monitoring, and defective area location. In the case of the Columbus module, a total of 12 ultrasonic transducers were located on the Columbus Shell and the impact localization accuracy was about 0.4 metres.

Prosser obtained acoustic emission signals created by impact sources in thin aluminum and graphite/epoxy composite plates. In his thesis, he also gave the characteristics of the impact signals created by the penetration and non-penetration impact failure. [Prosser *et al*, 1999].

Hypervelocity impact failure modes can be recognized by the characteristics of the impact signals. Wavelet transform and other signal-processing methods can extract the differences between varied factors. A data flow diagram (see Figure 3.1-1) shows the function of individual parts in an impact monitoring system. [Dae-Un Sung *et al*, 2002].

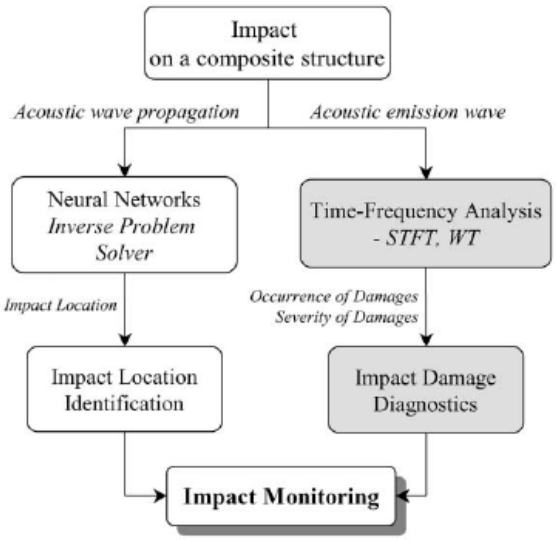

Figure 3.1-1 Data flow of monitoring system

3.1.4 Demands on the spacecraft

In the particular case of a large metallic structure like the ESA Columbus Module, 2 to 4 ultrasonic sensors should be mounted on the pressure containment wall for the purpose of generating signals to check the proper functioning of the system. The total mass of such a system is estimated to be 3.4 Kg, and the continuous power consumption to be 20 W.

3.1.5 Environmental robustness

AE monitoring systems can withstand the impact and vacuum environment whereas their performance under high/low temperature should be improved through special design. Signal collection may be disturbed by electromagnetic noise and therefore specific measures should be developed.

3.1.6 References

Chen, J.C., *Wideband Source Localization Using Passive Sensor Arrays*, Dissertation for Degree of Doctor of Philosophy in Electrical Engineering, University of California, Los Angeles, 2002.

Dae-Un Sung, Hun-Gou Kim, and Hang-Sun Hong, *Monitoring of impact damages in composite laminates using wavelet transform*. Composites Pats B, Vol. 33, p. 35-43, 2002.

Finkel, P.E., Miller, R.K., Finlayson, R.D., and Borinski, J., *Development of Fiber Optic Acoustic Emission Sensors*, Review of Progress in Quantitative Nondestructive Evaluation, Vol. 20, ed. Thompson and Chimenti, AIP Conference Proceedings 557, 2001.

Madaras, E.I., Prosser, W.H., and Gorman, M.R., *Detection of Impact Damage on Space Shuttle Structures Using Acoustic Emission*, AIP Conf. Proc. 9 April 2005, Volume 760, pp. 1113-1120.

Norske Veritas, *In-Orbit Non-Destructive Testing -Extension*, ESA / ESTEC Contract No. 8433/89/NL/PP (SC), DNV Report 92-3207 Rev. 2, 1992.

Price, D., *CSIRO's Aerospace Structural Health Management for the AAV Concept Demonstrator*, http://www.cip.csiro.au/AAV/demonstrator.htm (accessed 1 November 2005).

Promboo, Y., *Acoustic Emission Source Location*, Dissertation for Degree of Doctor of Philosophy, the University of Texas, 2000.

Prosser, W.H., Gorman, M.R., and Humes, D.H., *Acoustic emission signals in thin plates produced by Impact Damage*, Journal of Acoustic Emission, Vol. 17 (1-2), p. 29-36, June 1999.

Schafer, F., and Janovsky, R., *Impact Sensor Network for Detecting of Hypervelocity Impacts on Spacecraft*, IAC-04-IAA.5.12.2.04, 55th International Astronautical Congress 2004, Vancouver, Canada.

3.2 Accelerometers for Impact Shock Detection

3.2.1 Sensor description

Accelerometers can be used to detect the mechanical shock induced by a HVI on satellite structures. When a debris particle hits the outer shell of a spacecraft, a complex vibration environment is generated. Starting from the impact point, this includes in-plane and out-of-plane waves having different magnitude and frequency content. Such disturbances propagate far away from the impact location, depending on the load path found inside the structure (i.e. material, geometry, joints, etc.).

Accelerometers can be used not only to detect impacts, but also to estimate the impact features and criticality, since vibration characteristics in the “near field” (morphology,

amplitude, frequency content, speed of propagation, etc.) are strictly related to impact event and target local properties. To do this, it is essential to know the relations between impact parameters (debris density, shape, size, speed, obliquity, "near field" structural properties) and the generated shock [CISAS HVI team, 2006; Francesconi et al, 2007].

Nevertheless, sensors cannot be collocated too close to the exposed part of the structure, and so disturbance propagation (attenuation, reflection, superimposition, etc.) must be considered. Since it is strongly dependent on the structural properties in the "mid" and "far" field, an accelerator impact sensor system must be tailored to each specific application.

3.2.2 Development status

Accelerometers are widely used instrumentation for engineering and they are available in many different forms (detection principle, measuring range, bandwidth, size, mass). Even conditioning systems (charge amplifiers, voltage amplifiers) are widely available.

Boeing led development efforts to install 88 sensors on each wing of the orbiter Discovery. Sixty-six measure acceleration and impact data to gauge their strength and location. Tests have demonstrated these sensors can detect very small impacts. The sensors are highly sensitive and take 20,000 readings per second. This new network of sensors running along the wings provides an electronic nervous system that gives engineers a valuable way to monitor their condition. An added benefit of the impact sensors is their ability to detect orbital debris impacts while the shuttle is on orbit. The sensors are part of the Wing Leading Edge Impact Detection System, a new safety measure added for all future Space Shuttle missions.
For further information, see
http://www.boeing.com/defense-space/space/returntoflight/vehicleupgrades/wings.html

A low energy consumption sensor node for impact detection is currently under development: Invocon, Inc. has been awarded a NASA Phase 2 Small Business Innovation Research program to develop self-contained, miniaturized, piezoelectric sensory nodes with extremely low-power trigger modes that are synchronized within a radio frequency network. Each node will continuously monitor an accelerometer, acoustic emission sensor, or PZT element for an impact event, such as a micro-meteor impact. When a programmable threshold is exceeded, a low-latency signal acquisition circuit will capture the event as a digital waveform for post-processing and impact characterization including amplitude and time-of-arrival analysis. The innovative signal conditioning circuit design is capable of operation in the micro-watt range on average while constantly maintaining the capability to acquire and process very high frequency acoustic signals. Such performance can potentially provide operating lifetimes of 5 years on a single AA battery, or unlimited operation from scavenged power sources [Champaigne & Sumners, 2006].

3.2.3 Measurement capability

From a general point of view, accelerometer networks may be used for both impact detection and impact characterisation (see "sensor description" above)

Different sensor types exist to measure acceleration in the "near", "mid" and "far-field". Acceleration levels may go from 0.001 ms^{-2} to $2x10^{6}$ ms^{-2} and bandwidth may go from steady

acceleration to 200-250 kHz (sensor resonance around 1 MHz), depending on the sensor working principle (piezo-electric, piezo-resistive, etc.) and particular construction.

Laboratory impact tests have been carried out at CISAS hypervelocity facility. Al spheres (diameter ranging from 0.8 mm to 4 mm) impacted Al and CFRP thin rectangular plates and honeycombs (both single plate and plate assemblies with joints) at velocities between 2000 m/s and 5000 m/s [Pavarin *et al*, 2007]. Accelerations generated and propagated after such impacts have been recorded by shock accelerometer (Endevco, B&K and PCB shock sensors). The frequency and intensity of the transduced acceleration signal depends on the distance between the sensor and the impact location, on the impact velocity and debris mass. Moreover, using Wavelet Transform analysis, the type and speed of propagation of the waves can be identified [Bettella *et al*, 2007].

3.2.4 Demands on the spacecraft

The use of an accelerometers network would affect system resources in terms of (see technical data for details):

- Mass (of both accelerometers and wiring; on the latter point wireless systems are available, even to simplify integration problems).
- Power. Most accelerometers are passive detectors. Power demands are related to the conditioning system (amplifiers).
- Data handling. This is the most critical point, especially if acceleration signals have to be used for determining impact characteristics and criticality. Since the HVI footprint on signals is primarily related to the high frequency content, the sampling frequency should be kept high, at least at levels that are typical for pyroshock "near field" characterisation (well above kHz). This results in a huge amount of data to be stored and processed. Techniques to drastically reduce the data output are currently under development [Champaigne & Sumners, 2006].

3.2.5 Environmental robustness

Accelerometers should not be directly exposed to the space environment. Nevertheless they tolerate vacuum operations.

Temperature variations that are possible on orbit may affect the sensors calibration and it might be necessary to re-calibrate the measuring system at the expected working conditions in space.

No data are usually available about the interaction with the radiation environment.

3.2.6 References

Bettella, A., Francesconi, A., Pavarin, D., Giacomuzzo C., and Angrilli, F., *Application of wavelet transform to analyze acceleration signals generated by HVI on thin aluminum plates and all-aluminum honeycomb sandwich panels*, Hypervelocity Impact Symposium,

Williamsburg (Virginia USA), 23-27 September 2007, to be published in the International Journal of Impact Engineering.

Champaigne, K.D., and Sumners, J., *Low-power Electronics for Distributed Impact Detection and Piezoelectric Sensor Application,* IEEE 2006.

CISAS HVI team, *Inputs for the Impact Sensor System*, 24th IADC meeting, Tsukuba, 2006.

Francesconi, A., Pavarin, D., A., Giacomuzzo, C., Faraud, M., Destefanis, R., Lambert, M., and Angrilli, F., *Generation of transient vibrations on aluminum honeycomb sandwich panels subjected to hypervelocity impacts*, Hypervelocity Impact Symposium, Williamsburg (Virginia USA), 23-27 September 2007, to be published in the International Journal of Impact Engineering.

Pavarin, D., Francesconi, A., Destefanis, R., Faraud, M., Lambert, M., Bettella, A., Debei, S., De Cecco, M., Giacomuzzo, C., Marucchi-Chierro, P.C., Parzianello, G., Saggin, B., Ullio, R., and Angrilli, F., *Spacecraft disturbances induced by hypervelocity Impacts*, Hypervelocity Impact Symposium, Williamsburg (Virginia USA), 23-27 September 2007, to be published in the International Journal of Impact Engineering.

3.3 Impact Detection using Thermography

3.3.1 Sensor description

Thermography is a promising imaging technique that can be used to detect impacts in two different modes:

- Periodic inspections. This technique follows an appropriate schedule for periodic surface scanning, to determine if impacts occurred since the previous inspection. The method may require a suitable heat source to induce thermal waves inside the material, which are then sensed by an infrared camera. Differences in the structural cool down response caused by thermal properties changes may be finally associated to damages. Such a method is especially suited to detect delamination in composite panels, through a simple one-sided inspection.
- Continuous sampling. In principle, detecting impacts while they are occurring is possible since one of the consequences of HVI is a strong local heating taking place very close to the impact point. Such heating causes IR radiation emission that could be sensed by appropriate detectors, e.g. making thermal images of the surfaces exposed to the debris flux. It could even be argued that the amount of IR energy emitted may be related to the features of the impacting debris (material, size, shape, speed, etc.) after proper laboratory calibration.

The possibility of using both techniques is related to each specific configuration, since it depends on the thermal paths around the impact point (related to geometry, material type, thermal and optical properties), and the resulting decay time of the observable signal. Such decay time should be long enough to avoid unrealistic requirements for the detectors frame rate.

Typical specifications for a thermography camera are given in Table 3.3-1 [BFI Optilas, 2004].

Characteristics	Specifications
Manufacturer	BFI Optilas
Mass	1.2 kg
Power	> 10 W
Dimensions	14 cm × 11.4 cm × 11.4 cm
Operating temp.	-20°C to + 45°C
Sensitivity	0.08°C

Table 3.3-1 Technical specifications for the PV-320 camera by BFI Optilas (n.d.)

3.3.2 Development status

Thermal imaging systems are off-the shelf instrumentation for engineering ground-based applications, even though at the moment it's not evident that COTS cameras may be easily employed in space conditions.

Referring to the periodic inspection method, thermal inspection techniques have been studied in the last two decades [Smith, 1992; Walker & Workman, 1998] following the need of locating and quantifying the damage on aerospace parts made by composite material, which commonly exhibits negligible surface impact damages but large delamination throughout the thickness.

Thermographic techniques have been employed for damage detection during the ground inspection of the reinforced carbon-carbon (RCC) used for the wing leading edge of the Shuttle orbiter [Madaras *et al*, 2005]. The method demonstrated the ability of inspecting large areas in a relatively short time, being also valid for several applications to the Shuttle in preparation for return to flight, including for inspection of RCC panels during impact testing, and for between-flight orbiter inspections. A specific study [Howell *et al*, 2005] investigated the possibility of using thermal imaging during orbital conditions, accounting for the limitation of available mass, power, data handling and computation resources.

Referring to the continuous sampling method, it must be stressed that laboratory tests are needed to ascertain the possibility of recognizing and characterizing impacts from the thermal emission occurring during the event. The use of thermal imaging for measuring the radiation emitted during an HVI has been attempted [CISAS HVI team, 2006] on CFRP and Al-alloy bumpers, impacted at around 5 km/s with 2-3 mm Al-alloy projectiles. A temperature gradient around the impact point could be observed for CFRP bumper, but not for Al-alloy bumpers, because of the lower thermal inertia of the latter targets. The temperature gradient appears to be impact energy dependent. Even for plastic material, thermal gradients disappeared after around 40 s, suggesting the need of acquiring images at high frame rate, thus making the continuous sampling technique difficult to implement. Therefore, periodic inspection thermography is considered to be a more feasible option.

The possibility of combining thermography with an optical laser system has been explored through the development of the AIDA detector [Bunte *et al*, 2003]. This also enables the particle velocity to be determined. Laser diodes are used to produce a thin (~3mm) light sheet through which particles impacting the spacecraft must travel. As they pass through the sheet they scatter the laser light, which is picked up by a set of photodiode detectors. By using a set of two or more laser light sheets, the velocity of the particle can be determined by the difference in time and position of the light sheet crossings. Further information on laser velocity detection is available in Section 3.10.

3.3.3 Measurement capability

Different thermal detectors are available off-the-shelf, sensitive to a wide range of wavelengths, based on different technologies and having different resolution. Nevertheless, significant effort is needed for the space qualification of such instruments.

The modifications required to a commercial camera for being suitable for Space Shuttle missions operations are reported in [Gazarik *et al*, 2005]. The resulting camera is an uncooled microbolometer one, with spectral range of 7.5 to 13 μm and a 320 x 240 pixel focal plane array. The field of view is 24° x 18° with a minimum focus distance of 0.3 m. It has a thermal sensitivity of 0.06°C at ambient and can collect and store up to 600 frames of 14 bit integer data to built-in RAM at a maximum frame rate of 60 Hz. After collecting the data in RAM, the camera can then write to a removable compact flash memory card. The flash memory card will be used to transfer the data to an onboard computer for transmission to the ground for processing.

Finally, it should be noted that thermography is very promising to control the integrity of PVDF, MOS and Capacitance sensors (on debonding).

3.3.4 Demands on the spacecraft

The use of thermal imaging systems would affect system resources in terms of:

- Mass and Power.
- Size.
- To provide an external heat source for on-orbit inspection, the use of solar energy is suggested [Howell *et al*, 2005]. This approach reduces the system weight and power, but places an operational constraint on the measurement as the data must necessarily be taken during the daylight portion of the orbit.
- Data handling. This is related to the required frame rate, the area to be scanned, and the detector resolution (number of pixels).
- For IR measurements, the night part of a spacecraft orbit is preferable.

In view of these points, it is likely that thermal imaging systems will only be used on crewed spacecraft for the foreseeable future.

3.3.5 Environmental robustness

Thermal imaging systems should require protection from the environment. Commercial solutions have strict operating temperature ranges and the radiation environment may affect both performance and survivability of the system.

3.3.6 References

BFI Optilas (n.d.), *PV-320 Brochure 040703*, 2004.

Bunte, K., et al., *AIDA — An Advanced Impact Detector Assembly*, IN: International Astronautical Congress, Bremen, Germany, 29 September – 3 October, 2003.

CISAS HVI team, *Inputs for the Impact Sensor System*, 24th IADC meeting, Tsukuba, 2006.

Gazarik, M., Johnson, D., Kist, E., Novak, F., Antill, C., Haakenson, D., Howell, P., Jenkins, R., Yates, R., Rusty, Stephan, R., Hawk, D., and Amoroso, M., *Infrared On-orbit RCC Inspection with the EVA IR Camera: Development of Flight Hardware from a COTS System*, InfraMation: Infrared Camera Applications Conference, Las Vegas, NV, October, 2005.

Howell, P.A., Winfree, W.P., and Cramer, K.E., *Infrared On-orbit Inspection of Shuttle Orbiter Reinforced Carbon-Carbon Using Solar Heating*, in proc. SPIE Optics and Photonics, 31 Jul. - 4 Aug. 2005, 31 Jul-4 Aug 2005, San Diego CA USA.

Madaras, E.I., Winfree, W.P., Prosser, W.H., Wincheski, R.A., and Cramer, K.E., *Nondestructive Evaluation for the Space Shuttle's Wing Leading Edge*, 41st AIAA/ASME/SAE/ASEE Joint Propulsion, Tucson, AZ, July 10-13, 2005.

Smith, B.T., *Rapid detection and quantification of impact damage in composite structures*, NASA-CR-190367, 1992.

Walker, J.L., and Workman, G.L., *Study Methods to Standardize Thermography NDE*, NASA CR-1998-207358, 1998.

3.4 Calorimetry

3.4.1 Sensor description

3.4.1.1 Measurement principle

Calorimetric impact detection is based on the fact that a substantial part of the particle's kinetic energy E_{kin} is converted into heat when impacting the target. Consequently, the temperature of the target (in the following called "energy absorber") increases by ΔT which is measured by a contacted temperature sensor. This principle of calorimetric energy measurement is visualized in Figure 3.4-1.

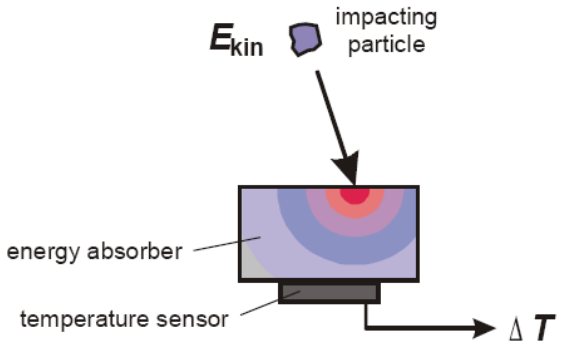

Figure 3.4-1 Calorimetric energy measurement

The ratio between measurable calorimetric heat and kinetic energy of the impacting particle is called the heat conversion efficiency

$$\eta_{conv} = \frac{E_{cal}}{E_{kin}} \qquad [3.4\text{-}1]$$

The knowledge about conversion efficiencies for hyper velocity impacts (HVI) is still fairly low. In general, some input energy is always lost through ejecta, impact plasma and radiation and thus cannot contribute to the measured heating of the calorimetric mass. Anyway, detector calibrations by HVI-tests will supply realistic values for the conversion efficiency.

For the idealized case of adiabatic heating, the deposed thermal energy E_{cal} leads to a temperature increase of

$$\Delta T = \frac{1}{m_A \cdot c_A} \cdot E_{cal} \qquad [3.4\text{-}2]$$

in thermal equilibrium, where m_A and c_A specify mass and specific heat of the energy absorber, respectively.

3.4.1.2 Detector design

Since an impact detector stage based on the calorimetric measurement principle provides the impacting particle's kinetic energy only, it always has to be combined with a second stage.

The AIDA (Advanced Impact Detector Assembly) detector concept is based on a two-stage approach, in which each stage can determine its measurands independently and with small uncertainties. The first stage will measure the velocity vector, the second stage the kinetic energy of the impacting particle. By using new detection methods, the detector assembly is supposed to be less affected by the space environment. This section addresses the calorimetric impact stage only.

Each module of the calorimetric detector operates a 16×16 array of miniaturized calorimeters covering a total detection area of about 33 square centimetres. Each calorimeter consists of an energy absorber and a temperature-measuring thermopile sensor contacted by thermal glue.

The core element of the sensor module is a two-dimensional thermopile array of 16×16 elements manufactured on a 4”-wafer. Figure 3.4-2 shows a photograph of the new thermopile array chip, which has a size of 58 mm × 58 mm.

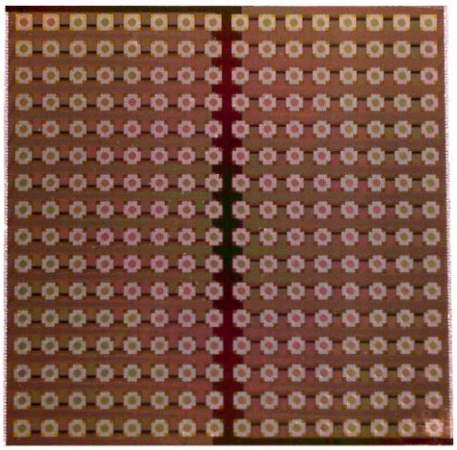

Figure 3.4-2 16×16 thermopile array

The calorimetric energy detector uses an array of thin metallic energy absorbers contacted to the underlying thermopile array by thermal glue. A plane plate absorber design has been chosen in order to guarantee uniform energy conversion efficiency all over the absorber surface, which is a precondition for accurate measurements requiring sensitivities as far as possible independent from impact location.

The individual absorber plates of the array are thermally isolated by small gaps of 50 μm width, thus their effective surface area measures 3.55 mm × 3.55 mm. All plates are connected at their edges by small joints to facilitate handling and mounting. As a drawback, these joints form a thermal bypass resulting in a small loss of sensitivity and some cross-talk between adjacent sensor elements.

Suitable absorber materials are metals of high thermal conductivity, like silver (Ag), gold (Au) or copper (Cu). For a given material and element size, the heat capacitance of the energy absorber is proportional to its thickness. Consequently, the calorimetric sensitivity of AIDA is adaptable to mission-specific needs by choice of an appropriate absorber plate thickness.

3.4.2 Sensor development status

A breadboard model of the AIDA calorimetric impact stage was developed within the scope of an assessment study [Bunte *et al*, 2006] released by ESA/ESTEC in order to review and improve in-situ measurement techniques for small particles. First information about this breadboard model was presented in [Kobusch *et al*, 2005]. The information provided in section 3.4.3 is based on the tests performed with the breadboard model which has reached a Technology Readiness Level of 4 (TRL4).

TRL5 will be reached in the framework of an activity funded by DLR. The aim of this activity is the development of a demonstration model of the calorimetric impact stage comprising the

manufacturing of the complete detector housing for 9 sensor modules and of one sensor module. In order to set up and test all required processes/technologies for the development of a flight model of the calorimeter the following tasks were performed:

- system design,
- semi-automatic gluing of a 16×16 element absorber array onto the thermopile array,
- optimisation of the electronic design.

The activity will be successfully finalised soon, and a follow-on project was initiated to build a flight model of the AIDA calorimeter. In the framework of this future activity it is planned to reach TRL8.

The possibility of combining calorimetry with an optical laser system has been explored through the development of the AIDA detector [Bunte *et al*, 2003]. This also enables the particle velocity to be determined. Laser diodes are used to produce a thin (~3 mm) light sheet through which particles impacting the spacecraft must travel. As they pass through the sheet they scatter the laser light, which is picked up by a set of highly sensitive photosensors. By using a set of two or more laser light sheets, the velocity of the particle can be determined by the difference in time and position of the light sheet crossings.

In the framework of a study funded by the German Federal Ministry of Economics and Technology a breadboard model of AIDA's velocity measurement stage was developed and tested [Bunte *et al*, 2008]. It was shown that particles with diameters down to 20 µm can be detected at impact velocities of 10 km/s.

Further information on laser velocity detection is available in Section 3.10.

3.4.3 Sensor measurement capability

Function, performance and behaviour of the AIDA calorimetric energy detector were investigated through different tests. The full test program included:

- Functional tests
- Performance and sensitivity tests
- Environmental tests
- Hyper velocity impact (HVI) tests

Where applicable, the tests made use of laser pulse heating in air or vacuum, which allows the deposition of defined heat energies on black-painted absorbers to simulate impact heating. Performance and sensitivity tests applied laser pulse heating in vacuum in order to determine sensitivity, sensitivity distribution, linearity, detection threshold and response time. Environmental tests investigated the behaviour to thermal loads, superposed illuminations, mechanical vibrations and electromagnetic radiation.

The following paragraphs focus on the most important tests with respect to the performance of the calorimetric measurement principle. All presented test results were obtained with calorimeter elements equipped with gold absorbers of 2.8 microns thickness.

According to Equation 3.4-2, the temperature increase of the impact-heated absorber, and thus the resulting calorimeter output signal, is principally proportional to the absorbed thermal energy. This linear measurement characteristic was experimentally verified by laser pulse heating in vacuum. Figure 3.4-3 plots the measured signal pulse heights against incident laser pulse energy on double-logarithmic scales.

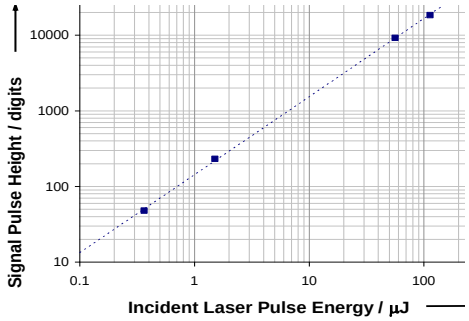

Figure 3.4-3 Calorimeter signal vs. input energy

The tested energy detector shows a linear signal response over an input energy range of about 300:1.

Hyper velocity impact (HVI) tests with the breadboard model were performed at the dust accelerator at the Max-Planck-Institute for Nuclear Physics at Heidelberg, Germany. Figure 3.4-4 shows the measurement characteristics of the tested calorimeter elements. In this double-logarithmic diagram, the measured signal pulse height is plotted against kinetic energy of the impacting particle. The noise-limited detection threshold of 4 digits and the 500 nJ kinetic energy of a candidate particle (10^{-14} kg at 10 km/s) are marked in the diagram. All detected HVI events had smaller energy values.

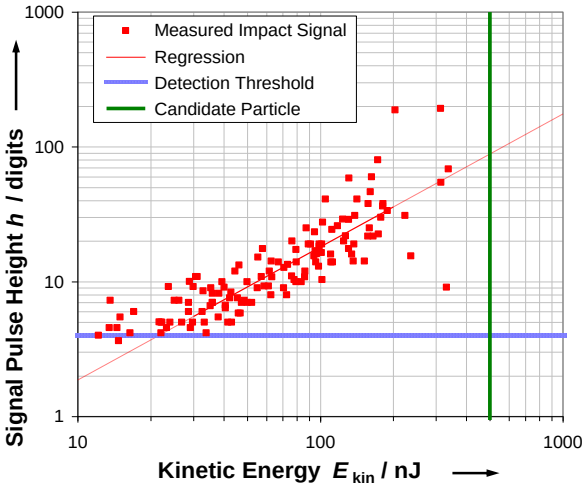

Figure 3.4-4 Measurement characteristics

The measured data points are scattered around a linear characteristics described by the plotted regression line derived from impact data for the mid-energy range from 20 nJ to 200 nJ. In this range, the measured data points are scattered over a factor of 2 to 3. The few data points above 200 nJ kinetic energy indicate stronger scattering at higher energies that possibly

results from impact penetration. Impact holes were actually found by microscopic inspection of the absorber surface.

The dynamic range of the presented calorimetric detector breadboard is about one order of magnitude in kinetic energy. The detection threshold is limited by noise, whereas the upper measurement range is related to the impact penetration of the thin metallic absorbers. If the array element spacing is constant, the dynamic range of this new type of space debris detector increases with absorber thickness. This relationship (which is valid under the assumption of proportionality between the particle diameter and the absorber thickness required to inhibit penetration) is sketched in Figure 3.4- 5.

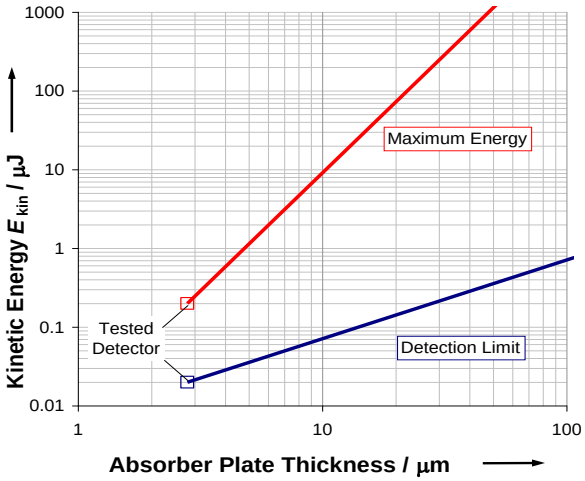

Figure 3.4-5 Expected upper and lower measurement limits for calorimetric detectors using gold plate absorbers of different thickness

By itself, calorimetry can only provide the impact energy, but not the particle's mass/diameter or velocity. Through the segmentation into relatively small sensor elements, it can also provide the impact location with a certain accuracy. Due to the time response of the calorimeter, the impact time cannot be measured with an accuracy sufficient to serve as potential stop signal of a time-of-flight measurement.

3.4.4 Demands on the spacecraft

The demands on the spacecraft listed in Table 3.4-1 were compiled for a calorimeter consisting of 16 sensor modules.

Resource	Description	Value
Mass	including housing, electronics, internal harness, etc. excluding harness and GSE	< 2 kg
Power	overall	< 10 W
Data rate	processing of impact events on-board the sensor expected	< 100 Kbps
TM/TC		downlink: < 1 KB/day uplink: < 512 Byte/day

Resource	Description	Value
Dimensions	max. for a detector consisting of 16 sensor modules; adaptation to specific spacecraft/missions possible	250 mm × 250 mm × 60 mm
Position	to be attached on the outer surface of the spacecraft; in the vicinity of critical equipment	N/A

Table 3.4-1 Resource requirements of the calorimeter

3.4.5 Environmental robustness

The AIDA calorimeter breadboard model has undergone some environmental testing [Kobusch *et al*, 2006-1]. No tests have been performed in domains where no susceptibility is expected.

Ionising Radiation: The influence of ionising radiation should be manageable by means of appropriate design and engineering. No tests were foreseen within the framework of this study, since no special susceptibility of AIDA-cal has to be expected.

Thermal Loads and Sun Illumination: Due to the calorimetric detection principle which relies on very small temperature changes, the susceptibility with respect to thermal loads and in particular to high thermal gradients is of major interest.

Thermal and illumination tests were part of the environmental tests. The test results show that thermal loads lead to variations of the sensor signal level. However, in most cases the impact signal can be deduced from the sensor output. Only very fast changes of the thermal loads (simulated by lamp illumination) lead to time periods where impact could not be detected.

An optimisation of the bandpass filter layout should help to minimise the susceptibility to fast changing thermal loads. Especially the eclipse – Sun passages should be no problem.

UV Radiation: AIDA-cal is expected to be not susceptible to UV radiation. Therefore, no respective tests were foreseen.

Radiated and Conducted Electromagnetic Interference: EMI should be manageable by means of appropriate design and engineering. Limited EMI testing was performed during the environmental tests campaign, which produced no evidence for special susceptibilities.

Plasma: AIDA-cal is expected to be not susceptible to the plasma environment. Therefore, no respective tests were foreseen.

Launch Vibrations: The AIDA-cal vibration tests were performed on qualification level. Although the breadboard model was not designed to withstand launch vibrations, damages were observed only in cases of pre-damage. Consequently, the susceptibility to launch loads should be manageable by means of appropriate design and engineering.

3.4.6 References

Bunte, K., et al., *AIDA — An Advanced Impact Detector Assembly*, IN: International Astronautical Congress, Bremen, Germany, 29 September – 3 October, 2003.

Bunte, K., *In-situ Detection and Material Returned from Space*, Proceedings of the 6th NoC Space Debris Co-ordination Meeting, Noordwijk, 6 October 2004.

Bunte, K.D., et al., *Assessment of In-situ Impact Detectors*, Final Report of the ESA/ESTEC Contract 17997/03/NL/JA, etamax space, Braunschweig, November 2006.

Bunte, K.D., et al., *Measurement of the Velocity Vector of small fast Particles in Space*, Final Report, etamax space, PTB, EMI, 16 January 2008.

Kobusch, M., et al., *Breadboard Model of a Calorimetric Impact Detector*, Proceedings of the 4th European Congress on Space Debris, ESA SP-587, Darmstadt, Germany, 18 April – 20 April, 2005.

Kobusch, M., et al., *AIDA-cal Test Report*, ESA/ESTEC Contract 17997/03/NL/JA, PTB, etamax space, Braunschweig, 2 February 2006.

Kobusch, M., et al., *Calorimetric Energy Detector for Space Debris*, 57th International Astronautical Congress, Valencia, Spain, 2 October – 6 October, 2006.

3.5 Optical Fibre Sensors

3.5.1 Sensor description

A fibre-optic cable consists of a core, a coat, a thin film of varnish and a plastic coating. The core and the coat of a glass fibre are mainly made of quartz glass. The light leading core transmits the signal. The coat also transmits light, but has a low refractive index. It causes a total reflection and thus contains the light signal within the core. The coating of the glass fibre is a protection against mechanical damage and normally has a diameter between 50 and 500 µm. Between the coat and the coating is a lacquer finish which is 2 to 5 µm thick, in order to protect the glass fibre against the damp atmosphere [Grattan, 1999; Staszewski, 2004].

Fibre optic sensors can be separated into two classes for discrete strain and temperature measurement: cavity-based designs and grating-based designs. Cavity-based designs utilize an interferometric cavity in the fibre to create the sensor. Examples include the extrinsic Fabry-Perot interferometer, the intrinsic or fibre Fabry-Perot interferometer, and all other etalon-type devices. Although such sensor designs have been utilized in a wide variety of applications such as in high temperature and electromagnetic interference environments, they do not allow for multiplexing capability in a single fibre, and thus may be limited for applications requiring a large number of sensors [Prosser, 2003].

Grating-based designs utilize a photo- or heat-induced periodicity in the fibre core refractive index to create a sensor whose reflected or transmitted wavelength is a function of this periodicity. The core of the fibre optic is illuminated by a pattern varied in space of short

wave ultraviolet laser light and the refractive index of the fibre optic locally changed. The light has enough energy to break open the highly stable silicon-oxygen-interconnections. That way the sensor is implemented into the fibre. Grating-based sensors (e.g. Fibre Bragg Gratings) can be easily multiplexed by using gratings of different wavelength as in the case of wavelength division multiplexing. Factors limiting the number of sensors in a single fibre include the limited bandwidth of the source as well as that supported by the fiber, and the range over which the physical parameter of interest is being measured [Grattan, 1999; Prosser, 2003; Kashima & Ozaki, 2001].

The nature and operation of Bragg grating sensors can be summarised as follows [Staszewski, 2004]:

- Bragg gratings are localized regions in a length of optical fibre. Many gratings can be imprinted along a single length. Each grating is typically 2 or 3 mm in length. These gratings constitute the sensors.
- The gratings have the property of reflecting light that is shone down the fibre, in a predetermined band of wavelengths. The grating themselves are periodic ripples in the reflective index in the fibre's core.
- As the fibre, and hence the grating is strained, the band of wavelengths at which the Bragg grating reflects is shifted. This strain can be induced quasi-statically, in which case the grating acts as a strain sensor, or can be dynamic such as the stress wave event caused by an impact.
- The sensor system operates by shining a broad range of wavelengths simultaneously down the fibre. The wavelength of the reflected light is detected in an opto-electronic module where wavelength shift is converted to an electrical signal that constitutes the raw sensor signal. This can then be captured and analysed using standard data capture equipment.

NASA identified Fibre Bragg Grating (FBG) sensor technology as the most promising future technology for structure monitoring [Prosser, 2003]. In fact, FBGs fulfil all demands placed on structure monitoring systems and are therefore most suitable for the monitoring of re-usable spacecraft.

3.5.2 Sensor development status

Approximately 10 years after the discovery of the FBGs, an efficient method was found to build FBGs by impressing the periodic refractive index modulation via ultraviolet light on the glass fibre. Nowadays, it is possible to produce FBGs in industrial scales.

Since the launch of the Fibre Bragg Gratings in 1995, the use of FBGs has increased exponentially in the fields of telecommunication and sensor technology. In the field of aerospace, ESA is using FBGs for the Ariane launcher, in order to supervise fibre-reinforced composites during its operation. The German ASTRA program included activities considering fibre optic sensor systems for temperature and strain measurement in a composite water tank [Reutlinger *et al*, 2000; Tennyson, 2004; Prosser, 2003; Smart Fibres Ltd.].

3.5.3 Sensor measurement capabilities

The use of fibre optic cables permits fast data transfer. Single mode fibres have a transmission rate of up to 1 Gbit/s. Fibre Bragg Gratings allow continuous and autonomous measures. The usage of fibre optic cables and Fibre Bragg Gratings makes it possible to undertake a real-time check of the structure during its operation [Smart Fibres Ltd.].

Structure monitoring systems based on FBGs in single mode fibres are also suitable for large structures. Single mode fibres have low optical signal decay. The signal needs to be amplified after a distance of more than 50 km [Reutlinger *et al*, 2000].

Using the fibre-optic sensor technology of FBGs, it is possible to place several thousand sensors in only one single mode fibre (see above) at a diameter of 125 µm. So FBG sensor systems are able to evaluate a large number of sensors in a small number of fibres. Thus wiring is reduced and the installation is facilitated. In addition glass fibres are actually already smaller and have less weight than electrical cables. Thus this technology is space-saving and lightweight and therefore can be brought into a spacecraft without large payload losses [Smart Fibres Ltd.].

Temperature and strain can be measured with the same sensor. In practice this can be both positive and negative. In order to be able to separate strain and temperature influences from each other, FBGs must be installed pair wise: one sensor measures strain and changes of temperature at the interesting structure, a second sensor in the proximity is attached in such a way that it does not take up strain but only measures the temperature [Smart Fibres Ltd.].

FBGs are able to operate from –270°C (strain measurement), alternatively –170°C (temperature measurement), up to +300°C. With so-called type II photo sensitive fibres the refractive index modulation remains permanent even up to 1000°C.

The measurement range, resolution and sample rate depend on the system itself (Fibre with sensors included and Signal Processing Unit). Typical values for these parameters are:

- Strain measurement range: up to 80.000 µm/m for one strain sensor
- Strain resolution: <5 µm/m
- Temperature measurement range: from cryogenic to 300°C
- Temperature resolution: <0.1°C
- Sample rate: up to 10 kHz feasible

3.5.4 Demands on the spacecraft

The possible usage of fiber optic sensors in re-usable spacecraft is limited by the temperatures that are reached when the spacecraft is re-entering the Earth's atmosphere. FGBs cannot be used at those spots of the re-usable spacecraft that are extremely thermally loaded, e.g. the wing leading edge, the nose and the parts at the rear side of the Space Shuttle, because they can endure up to 1000°C maximum, which is highly exceeded during re-entry. Only 3% of the surface reach such a high temperature during re-entry, the rest of the surface can be monitored [Grattan, 1999; Ecke *et al*, 2001].

The size, weight and power supply depend on the system. Here, typical values are:

- Dimensions (min.): 100 mm × 120 mm × 180 mm
- Mass: between 1.5 kg and 10 kg
- Power Supply: 9 to 36 V DC, 90 to 240 V AC (50-60Hz); Power Consumption ≤ 40 W max., ≤ 10W nominal

3.5.5 Environmental robustness

Dependent on the fixation of the fibre (with FBGs), either isolated from or mechanically coupled to the structure, local thermal or mechanical loads can be determined in the temperature range from -40°C to +190°C, and in the strain range from -0.1% to +0.3%. Short-term resolution and repeatability of the strain measurement amount to 5 με and 25 με, respectively.

They are even applicable under inhospitable circumstances, e.g. under effects of aggressive chemicals, radiation, high voltage or high temperatures. Fibre optics represent no risk in highly combustible environments and are chemically and thermally stable [Grattan, 1999; Ecke *et al*, 2001; Smart Fibres Ltd.].

FBGs do not need electrical energy and are therefore completely immune to interferences with electromagnetic fields.

3.5.6 References

Ecke, W., et al., *Fibre optic sensor network for spacecraft health monitoring*, Measurement Science and technology 12, p. 974-980, 2001.

Grattan, K.T.V., et al., *Optical Fiber Sensor Technology*, Vol. 3, 1999.

Kashima, S., and Ozaki, T., *Structural health monitoring using FBG sensor in space environment*, Proc. SPIE Vol. 4332, p.78-87, 2001.

Prosser, W.H., *Development of Structural Health Management Technology for Aerospace Vehicles*, NASA, 2003.

Reutlinger, A., et al., *Fiber optic sensor network for structural health monitoring*, Proc. SPIE Vol. 3986, p. 380-388, 2000.

Smart Fibres Ltd., UK, http://www.smartfibres.com

Staszewski, W., et al., *Health Monitoring of Aerospace Structures*, Wiley, 2004.

Tennyson, R., *SHM System for Detecting Foreign Object Impact Damage on Spacecraft*, Proceedings of the 2nd European Workshop on Structural Health Monitoring, 2004.

3.6 Resistor-based Detection

3.6.1 Sensor description

A resistor-based detector can detect a perforation hole generated by space debris impact in a manned space structure using a resistance film, which is attached to a pressurized wall with an insulator, as an area sensor. This detection system can simplify the wiring network when it is installed in a large space structure. The resistance value of a resistance film with a conductive condition is dependent on the distance between a measurement point and the perforation hole. This resistance value is measured by the direct current potential drop and then the perforation hole can be detected. Since the resistance film functions as an area sensor, even if it is destroyed locally, the destroyed area is not influenced in the detection system and the perforation hole can be detected without carrying out complicated analysis. If space debris perforates the pressurized wall, the pressurized wall and the resistance film can develop a contact through the impact damage. This method does not necessarily require simultaneous multipoint measurement at the instance of space debris impact because the resistance film and the pressurized wall have electrical continuity through the plastically deformed edge around the perforation hole.

3.6.2 Sensor development status

A Japanese project to develop a resistor-based detector was completed in March 2005 [Fukushige *et al*, 2005]. In this project, the results of detection tests with numerical analysis and pseudo-perforation hole demonstrated the effectiveness of the detection method using theoretical equations on infinite resistance film and a resistivity correction factor to consider shape effects (i.e. boundary condition effects). This method can be applied to any size and volume resistivity of a rectangular resistance film. The hypervelocity impact test demonstrated the effectiveness of the perforation detection system after an actual impact.

3.6.3 Sensor measurement capability

If the resistor-based detector is applied to a module on the International Space Station, the location resolution of 10 cm is small enough to decide an evacuation direction for the crew and a repair location for the structure. If a detection area density of $1.35 \times 10^{-2}/m^2$ is applied to the ISS surface area of 2200 m^2, the number of required measurement points is estimated to be 30.

3.6.4 Demands on the spacecraft

The required electric power is very small to detect the perforation hole because no current flows before the perforation and the signal processing after the perforation is also simple.

3.6.5 Environmental robustness

Environmental robustness of the resistor-based detection has not yet been tested. It can be expected that the resistor-based detection has some environment robustness because real time

processing of signals from the detector is not required and sampling rate of the detection is much smaller than other detectors.

3.6.6 References

Fukushige, S., Akahoshi, Y., Koura, T., and Harada, S., *Development of perforation hole detection system for space debris impact*, Proceedings of Hypervelocity Impact Symposium 2005, International Journal of Impact Engineering, Vol.33, 273-284, 2006.

3.7 Microwave Emission

3.7.1 Measurement principle

During a hypervelocity impact, a fraction of the projectile and target materials is evaporated and ionized (e.g. [Fechtig *et al*, 1978]). A plasma cloud is created almost instantaneously after the impact and expands into the surrounding vacuum. The plasma cloud consists of an ionized gas of projectile and target material and electrons. For example, [McDonnell *et al*, 1997; Ratcliff *et al*, 1997] provide empirical formulae for the evaluation of the charge Q produced during a hypervelocity impact, derived from impacts of micron-sized particles on targets. The charge yield equations are typically of the form:

$$Q \propto m^{\alpha} \cdot v^{\beta}$$

where m is the mass of the impacting particle and v is the impact velocity. α is most often assumed to be close to unity, while β is of the order of 3 to 4. Therefore, at increasing impact velocity, the ion yield increases strongly.

It is well known that light is emitted from this plasma, the so-called impact flash, induced by capture of electrons by ions and subsequent de-excitation processes in the atom. This flash has been observed e. g. by [Eichhorn, 1975]. One phenomenon that has not been investigated is the microwave emission that is emitted from the plasma. One possibility to explain the microwave emission is as follows: Immediately after impact, the plasma cloud is ejected in lateral direction from the impact site. Due to their much lower mass, the electrons are ejected at much higher velocities than the ions. Thus, effectively a charge separation takes place. Ions and electrons can then be seen as electric dipoles, oscillating with a frequency, the plasma frequency. The microwave emissions are in the GHz range. Such emissions have been experimentally observed by [Takano *et al*, 2000, 2002, 2005; Maki *et al*, 2002] and [Starks *et al*, 2006] report on microwave emissions from hypervelocity impact plasmas.

The microwave emissions from hypervelocity impact can be exploited to monitor hypervelocity impacts using antenna and RF pick-up coils.

3.7.2 Sensor description

A typical sensor is an antenna that is designed for operation at millimetre wavelengths or correspondingly, in the GHz frequency range, combined with amplifiers and a fast data

recorder. A convenient measurement window is 2 GHz to above 22 GHz. In order to increase the sensitivity of the antenna and directionality, a horn antenna can be used. As in this frequency range it is almost impossible to directly monitor the signal on an instrument, heterodyne detection scheme is used in order to transform the signal to a smaller bandwidth. [Maki *et al*, 2002] reports on using a heterodyne receiver in the 22 GHz band. He uses a low noise amplifier (LNA) in front of a mixer to obtain high sensitivity. The radio frequency (RF) band, the intermediate frequency (IF) band and the total gain of the receiving system are 22-23 GHz, 0-500 MHz and 82 dB, respectively. A digital oscilloscope with a sampling frequency of 1 GHz is used as a recording device.

3.7.3 Sensor development status

While microwave technology in general is well-established and related parts can be bought off-the-shelf, application of this sensor in the harsh environment of guns has not been practised much before. Development of this type of sensor to an industrial sensor requires a lot of effort, also, because microwave detection from hypervelocity impacts is not yet well understood theoretically and little has been done in the area of experimental calibration and testing of such a sensor.

3.7.4 References

Eichhorn, G., *Measurement of the light flash produced by high velocity particle impact*, Planet. Space Sci., 23, pp. 1519-1525, 1975.

Fechtig, H., Grün, E., and Kissel, J., *Laboratory Simulation* in: Cosmic Dust, edited by J.A.M. McDonnell (Wiley, Chichester), pp. 607-669, 1978.

Maki, K., Takano, T., Yamori, A., et al., *Detection of microwave emission in hypervelocity impact on aluminium*, Asia-Pacific Microwave Conference (APMC'02), Kyoto, 2, pp. 1327-1330, THOF83, November 2002.

McDonnell, J.A.M., McBride N., and Gardner, D.J., *The Leonid Meteoroid Stream: Spacecraft interactions and Effects* in: Proceedings of the Second European Conference on Space Debris, Darmstadt 1997, edited by B. Kaldeich-Schürmann and B. Harres (ESA Publication Division, Noordwijk), pp. 391-396, 1997.

Ratcliff, P.R., Burchell, M.J., Cole, M.J., et al., *Experimental measurements of hypervelocity impact plasma yield and energetics*, Int. J. Impact Engineering, 20, pp. 663-674, 1997.

Starks, M.J., Cooke, D.L., Dichter, B.K., Chhabildas, L.C., Reinhart, W.D., and Thornhill, T.F., *Seeking radio emissions from hypervelocity micrometeoroid impacts: Early experimental results from the ground*, International Journal of Impact Engineering, Vol.33, 781-786, 2006.

Takano, T., Murotani, Y., Toda, Y., et al., *Microwave generation due to hypervelocity impact*, 51th IAF Congress, IAA-00-IAA.6 .5.07, Brazil, October 2000.

Takano, T., Murotani, Y., Maki, K., et al., *Microwave emission due to hypervelocity impacts and its correlation with mechanical destruction*, J. Appl. Phys., 92(9), 5550-5554, November 2002.

Takano, T., Maki, K., Soma, E., Ohnishi, H., Ishii, K., Chiba, S., Fujiwara, A., and Yamori, A., *Material Dependence Of Microwave Emission Due To A Hypervelocity Impact*, Proceedings of the Fourth European Conference an Space Debris, Darmstadt, Germany, 18-20 April 2005 (ESA SP-587, August 2005).

3.8 Surface Inspection Cameras

3.8.1 Sensor description

Surface inspection cameras operate by taking a series of digital still images of a surface over a period of time and transmitting the images to Earth for analysis. New impact sites are identified simply by comparing the images. The technique can be combined with shock sensors or accelerometers to record the time of impact, and possibly to aid in the determination of impact velocity.

The transmission of detailed pictures back to Earth does of course place a burden on the telemetry systems of the host spacecraft. To reduce the data transfer, a proportion of the analysis can be performed using on-board processors. However, this is at the expense of an increase in the mass and power of the system.

3.8.2 Sensor development status

One method to inspect the surfaces of a spacecraft is for a small observation satellite to orbit the host spacecraft (i.e. untethered). It does, however, require its own spacecraft bus, propulsion systems etc. The lifetime of this free-flying “eyeball” is limited by the amount of propellant that it can carry. On exhaustion of its resources, or in the case of failure, the satellite then becomes a collision risk to the host spacecraft and itself a piece of space debris. There is also the possibility that particulates from the propulsion system of the eyeball satellite may contaminate surfaces on the host.

The LEMUR (Limbed Excursion Mobile Utility Robot) program at NASA’s JPL has produced a sub-5kg robot capable of moving independently around a surface [Kennedy *et al*, 2001]. This program is concentrating primarily on robots for very large structures, such as the International Space Station.

JAXA, the Japanese space agency, has experimented with a body-mounted CCD camera on board its Space Flyer Unit (SFU) and Experimental Test Satellite VII (ETS-VII). Details of another Japanese surface inspection system, which has been proposed for launch, are outlined in Table 3.8-1 [Hirayama *et al*, 2004]. This is an example of a CCD camera that would be mounted on the main body of the host spacecraft and would be capable of identifying impact craters of 0.5 mm or greater, corresponding to a particle size of 0.1 mm or above.

Characteristics	Specifications
Mass	> 10 kg
Field of view	1m × 1m
Minimum resolution	2000 × 2000 pixels
Magnification factor	× 10
Colour	Monochrome
Data	8 bit

Table 3.8-1 Technical specifications for a body-mounted surface inspection CCD camera

The NASA Space Shuttle uses an Orbiter Boom Sensor System (OBSS) to scan the leading edges of the wings, the nose cap, and other parts of the vehicle for impact damage soon after each lift-off and before landing. This system has been in use since STS-114 (July 2005). The purpose of the early inspection is to detect any potential critical damage to the thermal protection system of the vehicle caused by launch debris. The purpose of the late inspection is to detect any critical damage received from micro-meteoroid or orbital debris impacts. The OBSS is a 15 m long boom terminating in an instrumentation package that can be grappled by the Remote Manipulator System of NASA's Space Shuttle spacecraft. If flight engineers suspect potential damage to the areas scanned, more detailed or focused scans can be performed. If critical damage is detected with the OBSS, the crew may attempt a repair via a spacewalk, or if the damage is not repairable, the crew will dock with the International Space Station and await a rescue mission. The OBSS has two instrumentation packages (Figure 3.8-1). Sensor package 1 consists of a Laser Dynamic Range Imager (LDRI) and an Intensified Television Camera (ITVC). Sensor package 2 contains a Laser Camera System (LCS) and a digital camera (IDC). The sensors can resolve damage at a resolution of a few millimetres, and can scan at a rate of about 6 cm per second.

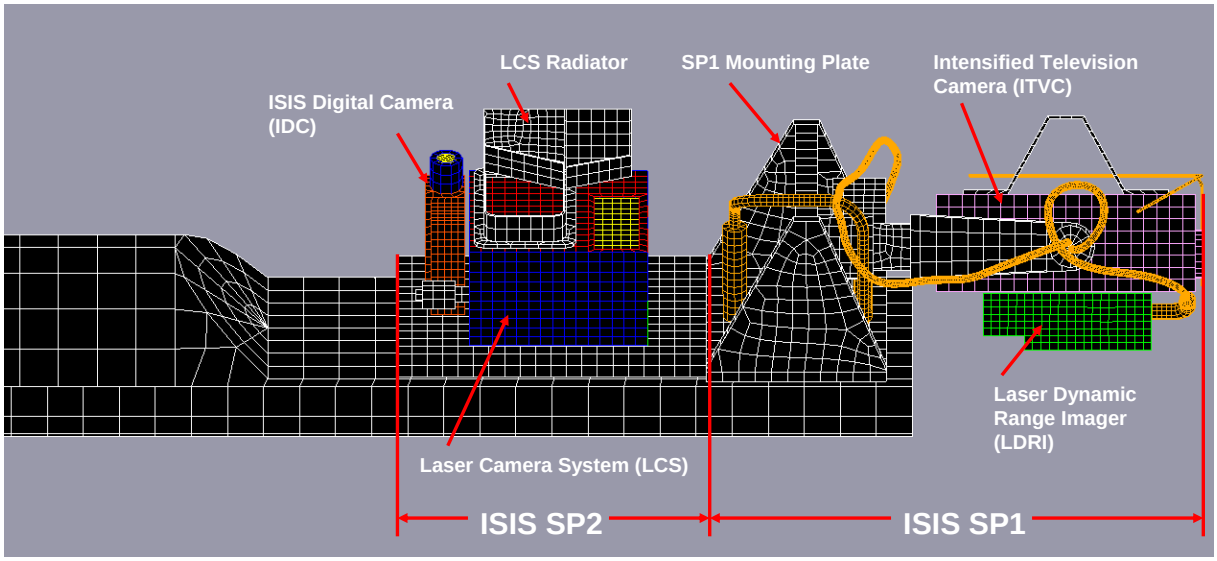

Figure 3.8-1 Orbiter Boom Sensor System (OBSS)

3.8.3 References

Hirayama, H., Hanada, T., and Yasaka, T., *In-situ Debris Measurements in MEO/HEO using Onboard Spacecraft Surface Inspection System*, Advances in Space Research 34 (5), 951–956, 2004.

Kennedy, et al., *LEMUR: Legged Excursion Mechanical Utility Rover*, Autonomous Robots, 11, 201–205, 2001.

4 Evaluation of Suitability of Sensor Systems

The suitability of the different impact sensor systems, for a given type of spacecraft mission, is summarised in Tables 4-1 to 4-4. Essentially, the tables evaluate the extent to which each sensor system can meet the requirements defined in Table 2.3-1. Table 4-5 provides definitions for the values contained in Tables 4-1 to 4-4.

Crew Vehicles	Acoustic	Acceleration	Thermography	Calorimetry	Fibre Optic	Resistor-based	Microwave	Camera
Availability	2	5	3	1	3	2	1	4
Range & Usefulness	3	3	4	3	3	3		2
Accuracy	4				4			3
Coverage S/C	3	2	3	2	4	4		4
Demands S/C	4	3	4	4	3	4		3
Environmental Rob.	5	2	1	4	4	3		3
Ease of Integration	4		3	1	1	2		2
Ease of Use	4	2	2	2	4	3		3
Cost	5	3	3	4	3			2
Overall	3.78	2.86	2.88	2.63	3.22	3	1	2.89

Table 4-1 Suitability of different impact sensor systems for crewed space vehicles

Crew-Re-entry Vehicles	Acoustic	Acceleration	Thermography	Calorimetry	Fibre Optic	Resistor-based	Microwave	Camera
Availability	2	5	3	1	3	2	1	4
Range & Usefulness	3	3	3	3	3	3		2
Accuracy	4				4			3
Coverage S/C	3	2	3	2	4	4		4
Demands S/C	4	3	4	4	3	4		3
Environmental Rob.	5	2	1	4	4	3		3
Ease of Integration	4		3	1	1	2		2
Ease of Use	4	2	2	2	4	3		3
Cost	5	3	3	4	3			2
Overall	3.78	2.86	2.75	2.63	3.22	3	1	2.89

Table 4-2 Suitability of different impact sensor systems for crewed re-entry vehicles

LEO Satellites	Acoustic	Acceleration	Thermography	Calorimetry	Fibre Optic	Resistor-based	Microwave	Camera
Availability	2	5	3	1	3	2	1	4
Range & Usefulness	3	3	3	3	3	3		2
Accuracy	4				4			3
Coverage S/C	4	3	3	2	4	4		4
Demands S/C	4	3	4	4	3	4		3
Environmental Rob.	5	2	1	4	4	3		3
Ease of Integration	4		3	1	1	2		2
Ease of Use	4	2	2	2	4	3		3
Cost	5	3	3	4	3			2
Overall	3.89	3	2.75	2.63	3.22	3	1	2.89

Table 4-3 Suitability of different impact sensor systems for unmanned LEO satellites

GEO Satellites	Acoustic	Acceleration	Thermography	Calorimetry	Fibre Optic	Resistor-based	Microwave	Camera
Availability	2	5	3	1	3	2	1	4
Range & Usefulness	3	3	3	3	3	3		2
Accuracy	4				4			3
Coverage S/C	4	3	3	2	4	4		4
Demands S/C	4	3	4	4	3	4		3
Environmental Rob.	5	1	1	3	3	2		2
Ease of Integration	4		3	1	1	2		2
Ease of Use	4	2	2	2	4	3		3
Cost	5	3	3	4	3			2
Overall	3.89	2.86	2.75	2.5	3.11	2.86	1	2.78

Table 4-4 Suitability of different impact sensor systems for unmanned GEO satellites

	1	2	3	4	5
Availability	Concept only	Under development	Developed; not flown	Flown; no supplier	Flown; ≥ 1 supplier
Range & Usefulness	1 data parameter	2 data parameter	3 data parameter	4 data parameter	≥ 5 data parameter
Accuracy	≥ 100% error margin	50% - 100% error margin	20% - 50% error margin	5% - 20% error margin	≤ 5% error margin
Coverage S/C	Partial cover; 1 surface only	Partial cover; high risk surfaces	Partial cover; all external surfaces	Full cover; high risk surfaces	Full cover; all external surfaces
Demands S/C	≥ 10% of nominal mission	5% - 10% of nominal mission	2% - 5% of nominal mission	1% - 2% of nominal mission	≤ 1% of nominal mission
Environmental Rob.	Sensitive to > 3 environmental factors	Sensitive to 3 environmental factors	Sensitive to 2 environmental factors	Sensitive to 1 environmental factors	Resistant to environment
Ease of Integration	Complex – e.g. active sensors	< ------ >	Intermediate	< ------ >	Simple – e.g. passive sensors
Ease of Use	Requires operator	< ------ >	Semi-automated	< ------ >	Fully automated
Cost	≥ 10% of nominal mission	5% - 10% of nominal mission	2% - 5% of nominal mission	1% - 2% of nominal mission	≤ 1% of nominal mission
Overall	Not recommended	Possible (if no better alternative)	Satisfactory	Good	Excellent

Table 4-5 Definitions of values in Tables 4-1 to 4-4

5 Conclusions

This document contains a review of technical solutions (available, under development or under study) for incorporating an impact sensor system as part of spacecraft health monitoring functionality. Such a sensor subsystem would have the purpose of detecting MMOD impacts on space vehicles and any anomalies that might result.
Each technical solution has been described referring to its working principle, its measurement capabilities and ranges, its potential application to space, its demands on the spacecrafts and its readiness at the state of the art.
The solutions have been evaluated in terms of their suitability for application on four different types of representative spacecraft mission, i.e. crewed space stations, crewed re-entry vehicles, unmanned GEO satellites and unmanned LEO satellites.
A summary of the findings is given below for all the options considered in the document.

Acoustic Emission sensors do not appear to have significant drawbacks, and currently have the broadest appeal for use as impact anomaly detectors on a wide range of spacecraft types.
While AE has been widely used in the damage detection fields, the technique also exhibits its potential ability for application to debris impact monitoring. The location of the impact and the identification of resultant damage modes have been preliminarily implemented for simple structures in the laboratory tests, but the application on real spacecraft structures will require attention and could be challenging in case of retrofit to an existing project.

Accelerometer networks may be used to sense vibrations produced by HVI-induced shocks on spacecraft structures. Even impact location and criticality may be assessed using adequate algorithms. Accelerometer networks require resources demanded of the spacecraft, in terms of the ability to manage signals with high frequency content. This point may be dealt with using two-stage (local and centralized) data handling systems.

Thermographic techniques may be used for inspecting large areas in a relatively short time: in particular, they have been applied for damage detection during the ground inspection of the TPS used for the wing leading edge of the Shuttle orbiter. Specific studies highlight the possibility of using thermal imaging even during orbital conditions, however technical issues still have to be addressed, accounting for the limitation of available mass, power, data handling and computation resources.

Impact detection with fiber optic sensors is still under development. The system components are already available and have been widely used in aerospace structures. This technology seems to be promising due to the ease of use, the coverage of the surface area and the environmental robustness. But due to the fact that it is difficult to integrate the fiber optics into the structure of the S/C, its application as impact sensors may be limited.

The use of the calorimetry technology as an impact sensor is at the beginning of the development process. It seems to be promising due to low costs and less demand on the spacecraft. But the ease of use, the low coverage of surface area and the complex integration will limit this technology as an option for impact sensor systems.

Resistor-based detectors may detect perforation holes generated by the space debris impact by using a resistance film. The detection system has the merit of simplifying the wiring network when it is installed in a large space structure. It is expected that resistor-based detection has

some environment robustness, because real time processing of signals from the detector is not required and sampling rate of the detection is much smaller than other detectors.

The monitoring of hypervelocity impacts by detecting microwaves emitted from impact generated plasma still demands considerable research and development activities in order to adopt microwave technology for this application and to yield a more comprehensive understanding of this impact effect.

Cameras and optical sensors have provided a means to detect micrometeoroid and orbital debris damage on the International Space Station and NASA Shuttle flights. Digital cameras and 3-dimension scanning systems have been used to determine the location and extent of damage. Cameras and optical systems are used to verify the existence of damage after other sensor systems have detected a possible impact. These systems generally rely on humans to interpret the images, to detect the presence of damage as well as locate and measure the damage.

6 List of Abbreviations

AAV	Ageless Aerospace Vehicle
A/D	Analog to Digital conversion
AE	Acoustic Emission
AIDA	Advanced Impact Detector Assembly
AIT	Assembly, Integration & Testing
Al	Aluminium
AO	Atomic Oxygen
ARGOS	Advanced Research and Global Observation Satellite
B&K	Brüel & Kjær
BLC	Ballistic Limit Curve
CCD	Charge Coupled Device
CCSDS	Consultative Committee for Space Data Systems
CFRP	Carbon Fibre Reinforced Plastic
CISAS	Centro Interdipartimentale Studi ed Attività Spaziali
CNES	Centre National d'Etudes Spatiales
CNRS	Centre National de la Recherche Scientifique
COTS	Commercial Off-The-Shelf
CPU	Central Processor Unit
CSIRO	Commonwealth Scientific and Industrial Research Organisation
DEBIE	Debris In-orbit Evaluator
DLR	Deutsches Zentrum fuer Luft- und Raumfahrt (German Aerospace Center)
DUCMA	Dust counter and mass analyser
EMC	Electromagnetic Compatibility
EMI	Electromagnetic Interference
ESA	European Space Agency
ETS	Experimental Test Satellite
EURECA	European Retrievable Carrier
EuTEF	European Technology Exposure Facility
EVA	Extra-Vehicular Activity
FBG	Fibre Bragg Grating
FOV	Field Of View
GIADA	Grain Impact Analyser and Dust Accumulator
GEO	Geosynchronous Orbit
GORID	Geostationary Orbit Impact Detector
GOSNIIAS	State Scientific Research Institute of Aviation Systems (Russian)
GSE	Ground Support Equipment
GSO	Geostationary Orbit
HEOS	Highly Eccentric Orbiting Satellite
HST	Hubble Space Telescope
HVI	Hyper Velocity Impact
IADC	Inter-Agency Space Debris Coordination Committee
IDC	ISIS Digital Camera
IDE	Interplanetary Dust Experiment
INP	Institute of Nuclear Physics
IR	Infra Red
ISA	Interstage Adapter
ISS	International Space Station
ITVC	Intensified Television Camera

IVA	Intra-Vehicular Activity
JAXA	Japan Aerospace Exploration Agency
JPL	Jet Propulsion Laboratory
LAAS	Laboratoire d'Architecture at d'Analyse des Systèmes
LAMA	Large Area Mass Analyzer
LCS	Laser Camera System
LDEF	Long Duration Exposure Facility
LDRI	Laser Dynamic Range Imager
LEMUR	Limbed Excursion Mobile Utility Robot
LEO	Low Earth Orbit
MDC	Munich Dust Counter
MEDET	Material Exposure and Degradation ExperimenT
MIS	Meteoroid Impact Sensor
MLI	Multilayer Insulation
MMOD	Micro-Meteoroid and Orbital Debris
M/OD	Meteoroid / Orbital Debris
MOS	Metal Oxide Semiconductor
MPI	Max Planck Institut
MSU	Moscow State University
MTS	Meteoroid Technology Satellite
MUSES	Mu Space Engineering Satellite
N/A	Not Applicable
NASA	National Aeronautics and Space Administration
NDE	Non Destructive Evaluation
OBSS	Orbiter Boom Sensor System
ODMCOrbiting Meteoroid & Debris Counting experiment	
ONERA	Office National d’Etudes et Recherches Aérospatiales
P/L	Payload
PROBA	Project for On-Board Autonomy spacecraft
PVDF	Polyvinylidene Fluoride
PZT	Lead Zirconate (piezoceramic)
RAM	Random Access Memory
RCC	Reinforced Carbon-Carbon
RDT&E	Research, Development, Test & Evaluation
RF	Radio Frequency
RSC	Rocket & Space Corporation
S/C	Spacecraft
SEM	Scanning Electron Microscope
SFU	Space Flyer Unit
SODAD	Système Orbital pour la Détection Active des Débris
SPADUS	Space Dust and Energetic Particle Experiment
STS	Space Transportation System
SUNSAT	Stellenbosch UNiversity SATellite
TBC	To Be Confirmed
TBD	To Be Determined
TC	Telecommand
TM	Telemetry
TOF	Time Of Flight
TPS	Thermal Protection System
TRL	Technology Readiness Level

TUM	Technical University of Munich
UV	Ultra Violet
WG	Working Group

7 Notations

Section 3.4.1

E_{kin}	kinetic energy
E_{cal}	measurable calorimetric heat
η_{conv}	heat conversion efficiency
ΔT	change in temperature
m_{A}	specify mass of the energy absorber
c_{A}	specific heat of the energy absorber

Section 3.6.3

r_p	minimum detected perforation hole size
r_d	distance between measurement points

Section 3.7

Q	charge
m	mass of the impacting particle and
v	impact velocity

Appendix A – Development and Flight Status of Impact Sensor Systems

Sensor type	Developer	Sensor name	RDT&E cost	Sensor maturity	Flown?
Acoustic sensor	NASA	PINDROP		Developed	No
	University of Rome	ISIS		Developed	No
	EMI	Impact Sensor Network		Under development	No
	CSIRO	Aerospace Structural Health Management for the AAV Concept Demonstrator		Under development	No
On orbit surface inspection - Free-flying "eye-ball"				Has something been developed or flown to support ISS?	
On orbit surface inspection - Mobile robotic scanner	NASA	Limbed Excursion Mobile Utility Robot (LEMUR)		Under development	No
On orbit surface inspection - Body-mounted camera	JAXA?	Cameras on JAXA's Space Flyer Unit (SFU) and Experimental Test Satellite (ETS-VII)		Developed	Yes
	JAXA	Onboard Spacecraft Surface Inspection System		Proposed?	No
Calorimetry		Advanced Impact Detector Assembly (AIDA)		Under development	No
Thermography		Flown as astronomical payloads to detect and study distant objects		Developed (for long range observations)	Yes (but not for debris detection)
		Advanced Impact Detector Assembly (AIDA)		Under development	No
Structural health monitoring		None?		Proposed?	No?

Appendix B – Summary Description of Impact Sensor Technologies

Sensor type	Impact detection technique	Sensor construction
Acoustic sensor	Patches bonded to spacecraft surfaces detect impact-generated acoustic shock waves. Triangulation (using signal time differences) determines impact location.	Piezoelectric materials - i.e. piezoceramics such as lead zirconate (PZT) or piezoelectric polymers such as PVDF.
On orbit surface inspection - Free-flying "eye-ball"	High resolution camera scans surface of spacecraft and takes digital stills.	A small observation satellite (free-flying "eye-ball") orbits the host spacecraft taking pictures
On orbit surface inspection - Mobile robotic scanner	High resolution camera scans surface of spacecraft and takes digital stills.	A small robot moves freely over the surfaces of a host spacecraft taking pictures. Similar concept to the free-flying "eye-ball", but lower collision risk
On orbit surface inspection - Body-mounted camera	High resolution camera scans surface of spacecraft and takes digital stills.	A CCD camera is mounted to the spacecraft body and takes pictures of different surfaces
Calorimetry	A particle impacting a spacecraft surface converts kinetic energy into heat energy which is absorbed by the surface and measured. The surface material must have low heat capacity and high thermal conductivity. It must also provide protection for the temperature sensor.	A single plate or plate array traps impactors and absorbs the energy. A lamella absorber comprises many thin plates joined together on a baseplate. A thermopile bonded to the surface measures the temperature change. An onboard processor converts this data back into the original impact kinetic energy.
Thermography	A particle impacting a spacecraft surface releases infra-red radiation that can be measured.	The infra-red radiation is recorded by an infra-red or thermal imaging camera. An on-board processor converts this data back into the original impact kinetic energy.
Structural health monitoring	A system to monitor strain and temperature changes in the external structure of a spacecraft. Strain and temperature changes are monitored by an optical fibre grid connected to a monitoring system. When an impact occurs, the optical path length of the fibre is changed and measured using interferometric techniques.	Optical fibre grid connected to a monitoring system. Fibres are non-conductive, immune to electromagnetic interference, and can be moulded to any shape

Appendix C – Measurement Capability of Impact Sensor Technologies

Sensor type	Particle type	Particle size	Particle speed	Particle trajectory	Impact KE / momentum	Impact time	Impact location	Impact crater/ hole size
Acoustic sensor	No	No	No	No	?	Yes	Yes	No
On orbit surface inspection - Free-flying "eye-ball"	No*	No*	No*	No*	No*	Yes	Yes	Yes
On orbit surface inspection - Mobile robotic scanner	No*	No*	No*	No*	No*	Yes	Yes	Yes
On orbit surface inspection - Body-mounted camera	No*	No*	No*	No*	No*	Yes	Yes	Yes
Calorimetry	No*	No	No	No	Yes	Yes	Yes	No
Thermography	No*	No	No	No	Yes	Yes	Yes	No
Structural health monitoring	No	No	No	No	?	Yes	?	?

*** Although not directly measurable, it may be possible to infer this characteristic (albeit approximately) from the other measured values**

**** Only if a particle hits the detector's sensing area. Impacts elsewhere on the satellite will not be observed.**

Appendix D – Detection Ranges / Thresholds of Impact Sensor Technologies

Sensor type	Sensing area	Particle size	Particle speed	Particle trajectory	Impact KE/ momentum	Impact crater/ hole size
Acoustic sensor	Sensor network could provide coverage of most of spacecraft	> 10 microns				
On orbit surface inspection - Free-flying "eye-ball"	Coverage of whole spacecraft					
On orbit surface inspection - Mobile robotic scanner	Coverage of most of spacecraft					
On orbit surface inspection - Body-mounted camera	Field of View = 1 m x 1 m	> 0.1 mm				> 0.5 mm
Calorimetry						
Thermography						
Structural health monitoring	Coverage of most of spacecraft	Depends on spacing of fibres				

Appendix E – Demands of Impact Sensor System on Spacecraft

Sensor type	Mass	Power requirement	Data requirement	On-board processing	AIT & Operations	Recurring cost (i.e. excl. RDT&E)
Acoustic sensor	< 1.5 kg	< 1 W				
On orbit surface inspection - Free-flying "eye-ball"	Several kilograms					
On orbit surface inspection - Mobile robotic scanner	5 kg					
On orbit surface inspection - Body-mounted camera	> 10 kg					
Calorimetry						
Thermography	1.2 kg	> 10 W				
Structural health monitoring	< 10kg	≤ 40 W				